

Determination of optimum Si excess concentration in Er-doped Si-rich SiO₂ for optical amplification at 1.54 μm

Oleksandr Savchyn,¹ Kevin R. Coffey,^{2,3} and Pieter G. Kik^{1,3,a)}

¹CREOL, College of Optics and Photonics, University of Central Florida, Orlando, Florida 32816, USA

²Advanced Materials Processing and Analysis Center (AMPAC), University of Central Florida, Orlando, Florida 32816, USA

³Department of Physics, University of Central Florida, Orlando, Florida 32816, USA

(Received 23 August 2010; accepted 1 November 2010; published online 18 November 2010)

The presence of indirect Er³⁺ excitation in Si-rich SiO₂ is demonstrated for Si-excess concentrations in the range of 2.5–37 at. %. The Si excess concentration providing the highest density of sensitized Er³⁺ ions is demonstrated to be relatively insensitive to the presence of Si nanocrystals and is found to be \sim 14.5 at. % for samples without Si nanocrystals (annealed at 600 °C) and \sim 11.5 at. % for samples with Si nanocrystals (annealed at 1100 °C). The observed optimum is attributed to an increase in the density of Si-related sensitizers as the Si concentration is increased, with subsequent deactivation and removal of these sensitizers at high Si concentrations. The optimized Si excess concentration is predicted to generate maximum Er-related gain at 1.54 μm in devices based on Er-doped Si-rich SiO₂. © 2010 American Institute of Physics. [doi:10.1063/1.3518476]

The development of on-chip photonic interconnects requires the development of a cost-effective Si-compatible light source.^{1–3} One actively investigated approach involves the use of Si-sensitized erbium in Si-rich SiO₂.^{4,5} Erbium, in its trivalent Er³⁺ state, exhibits sharp optical absorption and emission lines, one of which occurs at a wavelength of 1.54 μm . It is well known that the presence of excess silicon in Er-doped SiO₂ increases the Er³⁺ excitation cross section by several orders of magnitude^{6,7} and enables excitation in a wide wavelength range.^{4,8} Recently, it was demonstrated^{9,10} that Si excess-related luminescence centers (LCs) are the dominant sources of Er³⁺ sensitization in Si-rich SiO₂, as opposed to Si nanocrystals (NCs), which were previously thought to be the main sensitizers. Indirect Er-excitation through Si excess-related states was shown to occur even in as-deposited samples.⁸ The excitation of the first excited state of Er was characterized by a fast ($<$ 30 ns) transfer from LCs to the Er³⁺ first excited state (⁴I_{13/2}) as well as higher lying states, the latter resulting in the appearance of an additional slow contribution to the first excited state population.^{11,12} It was shown that low-temperature annealed Er-doped Si-rich SiO₂ exhibits a higher density of sensitized Er³⁺ ions as compared to its Si NC-containing counterpart⁹ and is therefore predicted to enable higher gain coefficients. To realize optimized devices based on this material, it is essential to determine the Si excess concentration that leads to the maximum concentration of sensitized Er³⁺. Relatively few studies consider the effect of Si excess concentration on the Er³⁺ emission.^{13–15} Furthermore, these studies focus predominantly on Er³⁺ emission intensities, rather than other relevant Er³⁺ characteristics, such as lifetime and excitation cross section, and often only consider high-temperature annealed samples. In this study, we determine the concentration of Si excess that maximizes the density of sensitized Er³⁺ ions for samples annealed at low temperature (not containing Si NCs) and high temperature (containing Si NCs) by taking

into account emission intensities, lifetimes, and excitation cross sections.

Er-doped Si-rich SiO₂ films (thicknesses of 107 ± 6 nm) containing 0.55 ± 0.05 at. % of Er as well as seven Si excess concentrations (C_{SiE}) in the range of 2.5–37 at. % were deposited onto separate silicon wafers by magnetron cosputtering. For each Si concentration, two sets of samples were prepared: samples annealed at 600 and 1100 °C (labeled LTA and HTA, for “low-temperature anneal” and “high-temperature anneal,” respectively) for 30 min in flowing Ar [flow rate of 65 SCCM (SCCM denotes cubic centimeter per minute at STP)]. All samples were subsequently passivated for 30 min in forming gas (N₂:H₂=95%:5%, flow rate of 65 SCCM) at 500 °C. Photoluminescence (PL) spectra were taken at room temperature under excitation with the 351 nm emission line of a Kr-ion laser (Spectra-Physics, BeamLok 2060). The irradiance at the sample surface was 2.4 W/cm². PL spectra were recorded with a charge-coupled device array (Andor, DU401-BR-DD) and a Ge-detector (Applied Detector Corp., 403S) in the spectral ranges of 400–1100 and 900–1750 nm, respectively, and were corrected for the system spectral response and sample thickness. All spectral PL measurements were done in the near-linear regime of PL versus power to minimize the effect of any nonlinear processes (excited state absorption and cooperative upconversion). PL traces were recorded using a photomultiplier tube (Hamamatsu 5509-73) in combination with a multichannel scaler (Stanford Research Systems, SR430). The spectral resolution in all PL measurements was \sim 10 nm, and the temporal resolutions were 0.64 and 2.56 μs for LTA and HTA samples, respectively. Lifetime measurements of the LTA sample with a Si excess concentration of 2.5 at. % did not provide sufficient signal-to-noise ratio due to the low Er³⁺ emission intensity from this sample. More information on the sample preparation and experimental techniques can be found in Refs. 9 and 10.

Figure 1(a) shows the PL spectra of LTA samples for different Si excess concentrations C_{SiE} on a logarithmic intensity scale. The spectra show three bands: a broad band

^{a)}Electronic mail: kik@creol.ucf.edu.

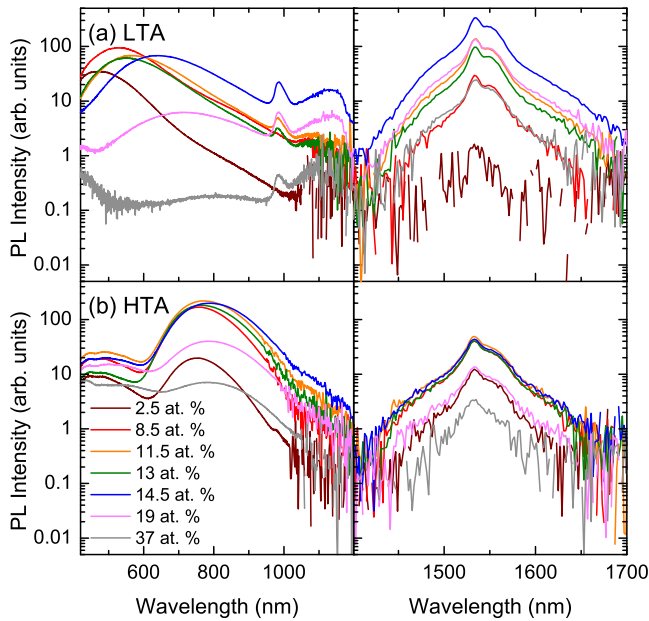


FIG. 1. (Color online) PL spectra of LTA (a) and HTA (b) samples with different silicon excess concentrations.

peaking in the range of 450–800 nm ascribed to Si excess-related LCs, and two narrow bands at 981 and 1535 nm corresponding to the Er^{3+} transitions ${}^4\text{I}_{11/2} \rightarrow {}^4\text{I}_{15/2}$ and ${}^4\text{I}_{13/2} \rightarrow {}^4\text{I}_{15/2}$, respectively. A fourth broad band peaking around 1130 nm is observed in LTA samples with $C_{\text{SiE}} > 13$ at. %. As C_{SiE} is increased, the LC PL spectra exhibit a significant redshift, suggesting that either interactions between adjacent LCs or possibly lattice strain can affect the LC energy levels. In addition, the full width at half maximum (FWHM) of the Er^{3+} PL spectrum at 1535 nm increases by $\sim 12\%$ as C_{SiE} is increased from 8.5 to 37 at. %, suggesting that the excess Si significantly affects the local Er^{3+} surroundings in low temperature processed samples. Figure 1(b) shows the PL spectra of the corresponding HTA samples, exhibiting three bands: a weak broad band peaking at ~ 450 nm corresponding to PL from LCs, a broad band at ~ 750 –800 nm related to PL from Si NCs, and Er^{3+} PL at 1535 nm. The Si NC PL spectrum shows a redshift with increasing C_{SiE} , which is commonly attributed to an increase of the NC diameter and a resulting reduced quantum confinement. No significant changes in the Er^{3+} PL FWHM are observed in these samples, suggesting that the Er^{3+} local environment is similar in all HTA samples. This could indicate that lattice relaxation occurs during the high-temperature anneal, or that the growth of Si nanocrystals leaves behind a significant number of sensitized Er^{3+} ions regions with a reduced local concentration of excess Si. Note that the Er^{3+} PL intensity at 1535 nm varies significantly as a function of C_{SiE} for both LTA and HTA samples, indicating a possible change in the density of sensitized Er^{3+} ions, the effective Er^{3+} excitation cross section, or the emission efficiency.

Figure 2(a) shows the dependence of the Er^{3+} PL intensity, integrated in the region of 1350–1700 nm (I , triangles) for LTA (open symbols) and HTA (solid symbols) samples. In both sample types, the Er^{3+} PL intensity initially rises as a function of C_{SiE} until concentrations of ~ 14.5 and ~ 11.5 at. % for LTA and HTA samples, respectively, after which the Er^{3+} PL intensity starts to decrease rapidly. In order to determine the origin of the intensity variation, decay

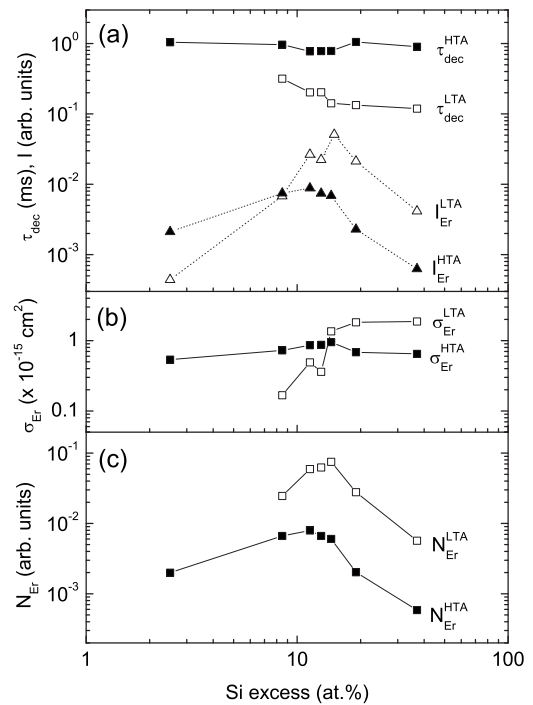


FIG. 2. (a) PL intensity of the Er^{3+} transition ${}^4\text{I}_{13/2} \rightarrow {}^4\text{I}_{15/2}$ integrated in the region of 1350–1700 nm I and the Er^{3+} PL decay time at 1535 nm τ_{dec} , (b) excitation cross section of the first excited state of Er^{3+} σ_{Er} , and (c) density of sensitized Er^{3+} ions N_{Er} of LTA and HTA samples as a function of Si excess concentration.

times τ_{dec} of the Er^{3+} PL at 1535 nm were determined by fitting the experimentally acquired decay traces with a stretched exponential function of the form $I(t) = I(0)\exp[-(t/\tau_{\text{dec}})^\beta]$, where β is the multiexponentiality factor. The value of β was found to be 0.72 ± 0.06 for all samples. The corresponding decay times are shown in Fig. 2(a) (τ_{dec} , squares) for LTA (open symbols) and HTA (solid symbols) samples. In LTA samples, the decay time decreases by a factor of ~ 3 as C_{SiE} is increased from 8.5 to 37 at. %. The corresponding increase of the total decay rate by more than 5000 s^{-1} is too large to be attributed to changes in the Er^{3+} radiative lifetime (typically 50–60 s^{-1} in SiO_2 based hosts¹⁶) and is most likely due to an increased nonradiative decay rate associated with the presence of electronic states introduced in the SiO_2 band gap by the presence of excess Si. In contrast, for HTA samples, the Er^{3+} decay time at 1535 nm shows a relatively constant value of $\sim 0.9 \pm 0.1$ ms for all C_{SiE} . This suggests that the high-temperature anneal leads to the removal of a significant fraction of such midgap states during the Si NC formation process.

The Er^{3+} first excited state excitation cross section (σ_{Er}) was determined based on the measured decay time (τ_{dec}) and rise time (τ_{rise}) (not shown) using the equation: $\sigma_{\text{Er}}\varphi = \tau_{\text{rise}}^{-1} - \tau_{\text{dec}}^{-1}$, where φ is the known pump photon flux ($\text{cm}^{-2} \text{ s}^{-1}$). The obtained σ_{Er} values are shown in Fig. 2(b). The values of σ_{Er} in LTA and HTA samples are found to be similar within a factor of 5 throughout the entire C_{SiE} range, supporting the presumption of a similar Er^{3+} excitation process in both sample types. For LTA samples, σ_{Er} is seen to increase by a factor of ~ 8 as C_{SiE} is increased from 8.5 to 37 at. %, whereas HTA samples exhibit a relatively constant σ_{Er} in the same C_{SiE} range. The origin of the rising σ_{Er} values in LTA samples as a function of increasing C_{SiE} is not

known; however, it should be noted that this change correlates with the appearance of a broad emission band at ~ 1130 nm, near the Er^{3+} 981 nm emission line [Fig. 1(a)]. The increase of the Er^{3+} excitation cross section in LTA samples with increasing C_{SiE} may be attributed to a combination of (a) the excitation of a single Er^{3+} ion by several LCs, (b) a C_{SiE} dependent variation in the electronic configuration of the LCs as inferred from the observed changes in the LC PL spectrum [Fig. 1(a)], (c) a change in the energy transfer process, or (d) the introduction of additional states at wavelengths >800 nm, through which the sensitization of Er^{3+} can occur directly into ${}^4\text{I}_{11/2}$ (981 nm) or possibly even into the ${}^4\text{I}_{13/2}$ (1535 nm) level of Er^{3+} . The last interpretation is in good agreement with our previous results^{11,12} where it was demonstrated that Er^{3+} can be indirectly excited by LCs into both the first excited state and the second excited state. Note that for Si excess concentrations below 11.5 at. %, the ER excitation cross-section in LTA samples is found to be lower than that in HTA samples. While the origin of this observation is not known, it could be related to a reduced energy transfer efficiency from LCs to Er in LTA samples due to the higher concentration of defects present in low-temperature annealed samples. It should be pointed out that at C_{SiE} values between 10–15 at.%, both sample types exhibit similar excitation cross sections. This finding is in agreement with our prior work⁹ on samples with a similar C_{SiE} of 12 at. %, in which σ_{Er} was found to be surprisingly weakly dependent on annealing temperature.

The values obtained in Figs. 2(a) and 2(b) enable the determination of a parameter proportional to the concentration of sensitized Er^{3+} ions N_{Er} . Modeling the Er^{3+} as a quasi-three level system, the Er^{3+} PL intensity I can be expressed as

$$I \propto \frac{\sigma_{\text{Er}} \varphi \tau_{\text{dec}} N_{\text{Er}}}{1 + \sigma_{\text{Er}} \varphi \tau_{\text{dec}} \tau_{\text{rad}}}, \quad (1)$$

where τ_{rad} is the radiative lifetime of the Er^{3+} transition at 1535 nm. This equation accounts for the onset of saturation of Er^{3+} emission intensity at the pump flux used. N_{Er} can thus be found in relative units, assuming that the Er^{3+} radiative lifetime τ_{rad} does not vary significantly. Figure 2(c) shows the resulting N_{Er} values. The maximum N_{Er} value occurs at $C_{\text{SiE}} \sim 14.5$ at. % and $C_{\text{SiE}} \sim 11.5$ at. % for LTA and HTA samples, respectively. Note that N_{Er} in LTA samples is a factor of ~ 4 – 14 higher than in HTA samples, depending on the Si concentration. Apparently, the high-temperature anneal reduces the fraction of sensitized Er^{3+} ions by an amount ranging from 75% to 93%. This dramatic reduction in N_{Er} is likely due to the reduction of the density of sensitizers resulting from the conversion of relatively homogeneously distributed excess Si atoms into Si nanocrystals, leaving behind regions with a reduced Si excess concentration. It should be noted that the analysis presented here assumes a fixed radia-

tive lifetime. However, changes in the local environment of the Er ions, for example through reconfiguration of Er–O bonds¹⁷ could lead to slight variations in the ${}^4\text{I}_{13/2} \rightarrow {}^4\text{I}_{15/2}$ radiative decay rate. This could affect the deduced values of N_{Er} ; however, these changes are expected to be relatively small compared to the observed dramatic variations in N_{Er} . Based on these observations, the presence of an optimum in N_{Er} as a function of Si excess concentration is attributed to an increase of the sensitizer density as C_{SiE} is increased, counteracted by a reduction in the sensitizer density associated with the formation of extended Si aggregates or nanocrystals. It should be noted that the optimum excess silicon concentration in LTA samples leads to the highest value of N_{Er} , optimal for high gain, as well as to an increased magnitude of σ_{Er} , suggesting that relatively low threshold pump powers can be achieved in the material.

In summary, the indirect excitation of Er in Si-rich SiO_2 films was investigated in the Si excess concentration range of 2.5–37 at. %. The Si excess concentration providing the highest density of sensitized Er^{3+} ions was demonstrated to be similar, independent of the presence of Si nanocrystals, and is, respectively, ~ 14.5 and ~ 11.5 at. % in samples without and with Si nanocrystals. The optimized Si excess concentration is anticipated to provide maximum Er-related gain at $1.54 \mu\text{m}$ in devices based on Er-doped Si-rich SiO_2 .

¹N. Daldosso and L. Pavesi, *Laser Photonics Rev.* **3**, 508 (2009).

²B. Jalali and S. Fathpour, *J. Lightwave Technol.* **24**, 4600 (2006).

³R. Soref, *IEEE J. Sel. Top. Quantum Electron.* **12**, 1678 (2006).

⁴M. Fujii, M. Yoshida, Y. Kanzawa, S. Hayashi, and K. Yamamoto, *Appl. Phys. Lett.* **71**, 1198 (1997).

⁵P. G. Kik, M. L. Brongersma, and A. Polman, *Appl. Phys. Lett.* **76**, 2325 (2000).

⁶M. Wojdak, M. Klik, M. Forcales, O. B. Gusev, T. Gregorkiewicz, D. Pacifici, G. Franzò, F. Priolo, and F. Iacona, *Phys. Rev. B* **69**, 233315 (2004).

⁷A. J. Kenyon, C. E. Chryssou, C. W. Pitt, T. Shimizu-Iwayama, D. E. Hole, N. Sharma, and C. J. Humphreys, *J. Appl. Phys.* **91**, 367 (2002).

⁸O. Savchyn, R. M. Todi, K. R. Coffey, L. K. Ono, B. R. Cuenya, and P. G. Kik, *Appl. Phys. Lett.* **95**, 231109 (2009).

⁹O. Savchyn, F. R. Ruhge, P. G. Kik, R. M. Todi, K. R. Coffey, H. Nukala, and H. Heinrich, *Phys. Rev. B* **76**, 195419 (2007).

¹⁰O. Savchyn, P. G. Kik, R. M. Todi, and K. R. Coffey, *Phys. Rev. B* **77**, 205438 (2008).

¹¹O. Savchyn, R. M. Todi, K. R. Coffey, and P. G. Kik, *Appl. Phys. Lett.* **93**, 233120 (2008).

¹²O. Savchyn, R. M. Todi, K. R. Coffey, and P. G. Kik, *Appl. Phys. Lett.* **94**, 241115 (2009).

¹³G. Franzò, E. Pecora, F. Priolo, and F. Iacona, *Appl. Phys. Lett.* **90**, 183102 (2007).

¹⁴H. S. Han, S. Y. Seo, J. H. Shin, and D. S. Kim, *J. Appl. Phys.* **88**, 2160 (2000).

¹⁵J. M. Sun, W. Skorupa, T. Dekorsy, M. Helm, and A. N. Nazarov, *Opt. Mater. (Amsterdam, Neth.)* **27**, 1050 (2005).

¹⁶M. J. A. de Dood, L. H. Slooff, A. Polman, A. Moroz, and A. van Blaaderen, *Phys. Rev. A* **64**, 033807 (2001).

¹⁷P. Noé, H. Okuno, J.-B. Jager, E. Delamadeleine, O. Demichel, J.-L. Rouvière, V. Calvo, C. Maurizio, and F. D'Acapito, *Nanotechnology* **20**, 355704 (2009).